Revisiting composite right-/left-handed transmission lines and symmetric couplers

B. Honarbakhsh*

Faculty of Electrical Engineering, Shahid Beheshti University, 1983969411, Tehran, Iran.

Abstract. The current research aimed to elaborate some hidden aspects of Composite Right-/Left-Handed (CRLH) Transmission Lines (TLs) and couplers. To this end, a complete and detailed dispersion analysis of an isolated CRLH TL was presented including lossless and lossy cases based on a conventional unit cell that was devised formerly. The dispersion analysis of the CRLH TLs was extended from conventional to accurate unit cells. The capability of TLs containing such unit cells to support the RLH waves was also demonstrated. A pure analytical strategy was then proposed for parameter extraction of the CRLH TLs and symmetric couplers based on accurate circuit models. According to the observations, once the loss parameters were included in the circuit model, no need would be felt to make use of curve fitting methods for extracting the parameters of the couplers under study.

1. Introduction

The main objective of this study is to shed light on some hidden aspects of a rather old but still attractive Transmission Line (TL) approach to the left-handed metamaterials. This valuable approach, first introduced in 2003 in a conference paper [1] and then further developed in a book in 2006 [2], has become a powerful engineering tool for designing advantageous microwave components since then [3–22].

The mentioned hidden aspects that have not been studied yet include a general dispersion analysis of lossy Composite Right-/Left-Handed (CRLH) TLs, clear decomposition of the dispersion relation of the CRLH TLs to the RH and LH regions, accurate analysis of the CRLH TLs based on the circuit model, precise parameter extraction of lossy CRLH TLs, and pure analytical strategy for parameter extraction of the symmetric CRLH couplers.

Two main issues are specifically revisited here: the dispersion analysis of a CRLH TL and parameter extraction of both CRLH TLs and symmetric edge couplers. Dispersion analysis of lossless CRLH TL was formerly carried out in [2,23]. However, in the lossless case, the selectivity of the correct branch of the phase constant has not been thoroughly elaborated. For the lossy TL, the analysis was restricted to the low-loss case. Parameter extraction was performed in [2,3] for a CRLH TL and a symmetric CRLH coupler, respectively. For both of these structures, only the lossless case was taken into consideration. It should be noted that in contrast to an isolated CRLH TL, the suggested strategy for extracting the circuit parameters of the coupler requires curve fitting methods, which is not purely analytic [2,3,9]. This in turn violates the purpose of the circuit model since curve fitting is potentially a time-consuming process

*. Tel.: +98 21 29904192
E-mail address: b_honarbakhsh@sbu.ac.ir (B. Honarbakhsh)

that may lead to loss of the correct phase response of the corresponding scattering (S-) parameters. Not only does the circuit model provide an intuitive description of the physical model but also serve as a valuable design tool. Therefore, its construction should take less time than a full-wave analysis of the complete structure.

The mentioned deficiencies will be later resolved in the present paper in the following sections. For instance, as shown in Section 2, it is not possible to uniquely determine the phase constant in a lossless CRLH TL. This situation is similar to the uniqueness theorem in electromagnetics that cannot be proven in a lossless medium [24]. Later in this study, a complete dispersion analysis of a lossy CRLH TL is provided, and the complex propagation constant is uniquely determined. In addition, it is observed that the lossless TL can be well described as the limiting case of the lossy TL. In Section 3, a general strategy is suggested to obtain the dispersion curves of a CRLH TL using an accurate circuit model of the corresponding unit cell. In Section 4, a method for parameter extraction of a CRLH TL is proposed based on the said unit cell. Finally, in Section 5, detailed parameter extraction of the symmetric CRLH edge coupler solely based on analytic expressions is presented. Through this research, the unit cell of all physical CRLH TLs is the same as that of the one proposed in [3] which involves cascading an Interdigital Capacitor (IDC) and a short-circuited Stub Inductor (SI). Full-wave simulations are carried out using Keysight$^{\circledR}$ Momentum.

2. Revisiting dispersion analysis

The unit cell of a conventional CRLH TL is depicted in Figure 1, where Z_s, Y_p, and δ are the series impedance, parallel admittance, and physical length, respectively [2]. The complex propagation constant of a TL including the cascading infinite number of such a unit cell can be represented by [25]:

$$\gamma = \lim_{\delta \to 0} \frac{1}{\delta^2} \sqrt{Z_s Y_p}, \tag{1}$$

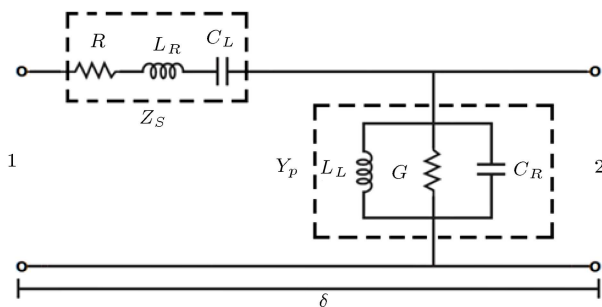which can be regarded as the dispersion relation. Subsequently, real and imaginary parts of the propagation

Figure 1. The unit cell of a conventional CRLH TL.

constant are derived as a function of angular frequency for lossless and lossy TLs. Note that due to the conservation of energy, the real part of the propagation constant must be non-negative. Additionally [2]:

$$\omega_{se} = 1/\sqrt{L_R C_L}, \qquad \omega_{sh} = 1/\sqrt{L_L C_R}, \tag{2a}$$

$$\omega_{\min} = \min\left(\omega_{se}, \omega_{sh}\right), \qquad \omega_{\max} = \max\left(\omega_{se}, \omega_{sh}\right). \tag{2b}$$

All the derivations of this section are at the level of high-school mathematics; thus, only the final results are included.

2.1. Lossless CRLH TL

In this case, the series impedance and parallel admittance are:

$$Z_{s,ll} = j\omega L_R + 1/\left(j\omega C_L\right),$$

$$Y_{p,ll} = j\omega C_R + 1/\left(j\omega L_L\right), \tag{3}$$

leading to:

$$\gamma_{ll}^2 = \left(\alpha_{ll} + j\beta_{ll}\right)^2 = f_1\left(\omega\right), \tag{4}$$

wherein the subscript "ll" stands for lossless. Also, according to [2], we have:

$$f_1 : \begin{cases} = -\left[\left(\omega/\omega_R\right)^2 + \left(\omega_L/\omega\right)^2 + \kappa\omega_L^2\right] \\ > 0, \quad \omega_{\min} < \omega < \omega_{\max} \\ < 0, \quad \text{otherwise} \end{cases} \tag{5}$$

Given that $\alpha_{ll} \geq 0$ and $\beta_{ll} \in \mathbb{R}$, it can be concluded that:

$$\alpha_{ll} = \begin{cases} +\sqrt{|f_1|}, & \omega_{\min} < \omega < \omega_{\max} \\ 0, & \text{otherwise} \end{cases} \tag{6}$$

and:

$$\beta_{ll} = \begin{cases} 0, & \omega_{\min} < \omega < \omega_{\max} \\ \pm\sqrt{|f_1|}, & \text{otherwise} \end{cases} \tag{7}$$

which define two pass-bands and one stop-band. As the first result of the present work, β_{ll} cannot be uniquely determined in the pass-bands resulting from neglecting the loss factor that permits both the inward and outward traveling waves to be valid solutions. Specifically, neither of these waves violates the conservation of energy. Only for completeness and integrity of the presentation, consider that the characteristic impedance of the lossless TL is obtained through the following equation:

$$Z_{c,ll} : \begin{cases} = \sqrt{Z_{s,ll}/Y_{p,ll}} = Z_R \sqrt{\frac{\omega^2 - \omega_{se}^2}{\omega^2 - \omega_{sh}^2}} \\ \in I, \quad \omega_{\min} < \omega < \omega_{\max} \\ \in +, \quad \text{otherwise} \end{cases} \tag{8}$$

Consequently, the corresponding reflection coefficient with *respect to a real characteristic impedance* is obtained as:

$$S_{11} \text{ (dB)} : \begin{cases} = 0, & \omega_{\min} < \omega < \omega_{\max} \\ < 0, & \text{otherwise} \end{cases} \qquad (9)$$

which shows a complete reflection at the stop-band. Note that at the stop-band, there is no thermodynamic loss. Of note, the attenuation constant is finite.

2.2. Lossy CRLH TL

In this case, the series impedance and parallel admittance are:

$$Z_{s,l} = R + Z_{s,ll}, \qquad Y_{p,l} = G + Y_{p,ll}, \qquad (10)$$

and the dispersion equation is:

$$\gamma_l^2 = (\alpha_l + j\beta_l)^2 = f_2(\omega) + jf_3(\omega), \qquad (11)$$

where the subscript "l" stands for lossy and:

$$f_2 = RG + f_1, \qquad (12a)$$

$$f_3 = RC_R\left(\omega - \omega_{sh}^2/\omega\right) + GL_R\left(\omega - \omega_{se}^2/\omega\right). \qquad (12b)$$

By defining Δ and ω_b as:

$$\Delta = \left[(\omega_{se} + \omega_{sh})^2 - RG\omega_R^2\right]\left[(\omega_{se} - \omega_{sh})^2 - RG\omega_R^2\right], \qquad (13a)$$

$$\omega_b = \sqrt{\left(RC_R\omega_{sh}^2 + GL_R\omega_{se}^2\right)/\left(RC_R + GL_R\right)}, \qquad (13b)$$

we have:

$$f_2 : \begin{cases} < 0, \Delta < 0, & \forall \omega \\ > 0, \Delta \geq 0, & \omega_1 < \omega < \omega_2 \\ < 0, & \text{otherwise} \end{cases} \qquad (14)$$

and:

$$f_3 \gtrless 0, \omega \gtrless \omega_b, \qquad (15)$$

where:

$$\omega_{1,2} = \frac{\sqrt{2}}{2}\sqrt{\left[(\omega_{se}^2 + \omega_{sh}^2) - RG\omega_R^2\right] \mp \sqrt{\Delta}}. \qquad (16)$$

In addition, we have:

$$\Delta < 0 \Leftrightarrow \left|\sqrt{\frac{L_R}{L_L}} - \sqrt{\frac{C_R}{C_L}}\right|$$

$$< \sqrt{RG} < \left|\sqrt{\frac{L_R}{L_L}} + \sqrt{\frac{C_R}{C_L}}\right|, \qquad (17a)$$

$$\omega_{\min} \leq \omega_b \leq \omega_{\max}. \qquad (17b)$$

Given that $\alpha_l \geq 0$ and $\beta_l \in \mathbb{R}$, solving Eq. (11) for α_l and β_l leads to:

$$\alpha_l = \frac{\sqrt{2}}{2}\left(f_2 + \sqrt{f_2^2 + f_3^2}\right) > 0, \qquad \forall \omega, \qquad (18)$$

and:

$$\beta_l = \begin{cases} -\frac{\sqrt{2}}{2}\sqrt{-f_2 + \sqrt{f_2^2 + f_3^2}}, & \omega < \omega_b \\ +\frac{\sqrt{2}}{2}\sqrt{-f_2 + \sqrt{f_2^2 + f_3^2}}, & \omega > \omega_b \end{cases} \qquad (19)$$

As a result, the line is considered LH for $\omega < \omega_b$ and RH for $\omega > \omega_b$. Hence, complete dispersion analysis of CRLH TLs is made possible through which the phase constant can be uniquely determined in any frequency band of interest. This is the second contribution of the present work.

2.3. Lossless CRLH TL as a limiting case of lossy CRLH TL

As a familiar technique, a lossless TL can be considered as a limiting case of the lossy TL when loss parameters approach zero. Note that the limit of ω_b does not exist when $(R, G) \to (0, 0)$ while Eq. (17b) guarantees that its limiting value is bounded by $\omega_{\min}$ and $\omega_{\max}$. Thus, at the limit, the sign of β_l cannot be determined when $\omega_1 < \omega < \omega_2$. In addition, Eqs. (12) and (16) will result in:

$$\lim_{(R,G)\to(0,0)} f_2 = f_1, \qquad \lim_{(R,G)\to(0,0)} f_3 = 0, \qquad (20a)$$

$$\lim_{(R,G)\to(0,0)} \omega_1 = \omega_{\min}, \qquad \lim_{(R,G)\to(0,0)} \omega_2 = \omega_{\max}. \qquad (20b)$$

Consequently,

$$\lim_{(R,G)\to(0,0)} \alpha_l =$$

$$\begin{cases} \frac{\sqrt{2}}{2}\left(f_1 + |f_1|\right), & \forall \omega \\ \sqrt{2}\,|f_1|, & \omega_{\min} < \omega < \omega_{\max} \\ 0, & \text{otherwise} \end{cases} \qquad (21)$$

and:

$$\lim_{(R,G)\to(0,0)} \beta_l = \begin{cases} +\frac{\sqrt{2}}{2}\sqrt{-f_1 + |f_1|}, & \omega > \omega_b \\ -\frac{\sqrt{2}}{2}\sqrt{-f_1 + |f_1|}, & \omega < \omega_b \end{cases} \qquad (22)$$

$$= \begin{cases} -\sqrt{2}\,|f_1|, & \omega < \omega_{\min} \\ 0, & \omega_{\min} < \omega < \omega_{\max} \\ +\sqrt{2}\,|f_1|, & \omega > \omega_{\max} \end{cases}$$

Therefore, in contrast to the lossless case, the phase constant of a lossy TL is, again, uniquely determined. Note that at the stop-band, the sign of β_l is unknown, while its value is known.

3. Revisiting CRLH TL unit cell

In the preceding section, dispersion analysis of CRLH TLs was precisely revisited through which some new aspects of the corresponding theory were addressed. The present section is devoted to the accurate study of the circuit model of physical CRLH TL unit cells. As observed, when the cell size is smaller than working wavelength, comprehensive realization of the CRLH TLs follows the theory and consequently, the reported
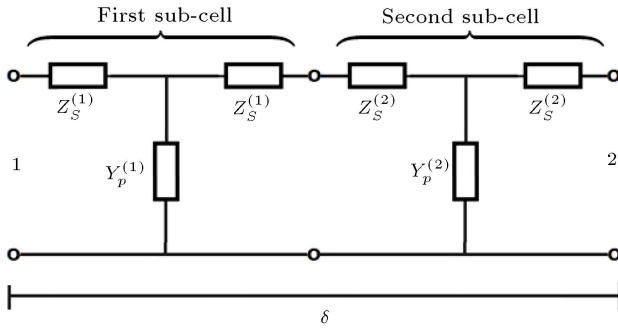
Figure 2. The unit cell of a CRLH TL consisted of cascading of two sub-cells.

results of the previous section will be applicable. To this end, note that the systematic method for the design and analysis of a CRLH TL is decomposing its unit cell into two cascaded sub-cells: one to provide series capacitance and the other to provide parallel inductance (Figure 2) [2].

In almost all such designs, each of the sub-cells can be modeled by a symmetric Π or T network. From the circuit theory viewpoint, the order of such a combination is greater than that of the conventional CRLH unit cell, hence not equivalent in the strict sense. However, the validity of such cells in providing the CRLH behavior is certain. As shown in this section, the desired equivalence holds when the cell size approaches zero. In this regard, the following steps based on MATLAB® Symbolic Computation Toolbox were considered. First, the *ABCD*-matrix of cascade combination of the T-networks corresponding to each sub-cell was computed. Then, upon using the said matrix and applying periodic boundary conditions, the determinantal equation governing the corresponding uniform TL was developed [2]:

$$AD - (A + D)\, e^{\gamma\delta} + e^{2\gamma\delta} - BC = 0. \qquad (23)$$

Next, the exponential functions in Eq. (23) were replaced by the first three terms of their Taylor's series expansion. This simplification is valid when the cell size is small compared to the working wavelength which is not only possible from the practical standpoint, but also required to ensure the homogeneity condition [2]. Finally, the leading term of the resulting polynomial in δ was extracted which included the desired dispersion equation. The derived dispersion relation exactly matches that of the conventional CRLH unit cell with:

$$Z_s^{(eq)} = \sqrt{\frac{2}{3}}\left(Z_s^{(1)} + Z_s^{(2)}\right),$$

$$Y_p^{(eq)} = \sqrt{\frac{2}{3}}\left(Y_p^{(1)} + Y_p^{(2)}\right), \qquad (24)$$

where the superscript "*eq*" stands for "equivalent" and:

$$Z_s^{(1)} = R^{(1)} + j\omega L_s^{(1)} + 1/\left(j\omega C_s^{(1)}\right),$$

$$Y_p^{(1)} = G^{(1)} + j\omega C_p^{(1)}, \qquad (25a)$$

$$Z_s^{(2)} = R^{(2)} + j\omega L_s^{(2)},$$

$$Y_p^{(2)} = G^{(2)} + j\omega C_p^{(2)} + 1/\left(j\omega L_p^{(2)}\right). \qquad (25b)$$

As another contribution of the present work, it is rigorously shown that the developed TL theory is applicable to the physical realization of CRLH TLs.

4. Revisiting parameter extraction of CRLH transmission lines

Thus, the formation of a CRLH TL has been proved based on the previously reported structures. In the present section, an accurate and general method is presented to derive the corresponding dispersion characteristic and circuit parameters from either the measured results or full-wave simulation. In [2], an analytic method was proposed for parameter extraction of the CRLH TLs. The attained circuit model is beneficial in two terms. First, it simplifies the design and analysis of such TLs and second, the dispersion analysis of the line becomes straightforward. In this respect, three simplifications were taken into account. First, the devised closed-form formulas are based on the lossless line. Second, the circuit elements are extracted at a single frequency. Third, the unit cell of the physical TL is forced to be equivalent to the lossless version of Figure 1.

It should be noted that the last simplification is not possible in a strict sense, as already explained in Section 3. The benefits of the circuit model can be preserved by incorporating the loss parameters without overloading the computational resources. According to the previous section, the accurate circuit model exactly matches its conventional counterpart at the limit, hence no need for the conventional circuit enforcement to the physical model. In addition, even when low-loss dielectrics are exploited in the physical realization of the CRLH TLs, the values of lossy elements are not necessarily negligible. Obviously, CRLH TLs are potentially suitable radiators to be utilized as antennas, whose applications have been justified long ago [2]. In such cases as the series resistance in the circuit model, proper modeling of the radiation loss gains significance.

Of note, doing the dispersion analysis based on the accurate circuit model is straightforward. For this purpose, first, Eq. (23) should be transformed into a quadratic equation in variable X with $X = e^{\gamma\delta}$ and then, since $\alpha_{ll} \geq 0$, the desired solution should be selected such that $|X| \leq 1$. This procedure is both general and accurate. Another simplification that has been followed thus far is restricting the parameter extraction to a single frequency. Full-wave analysis of a unit cell is not computationally costly

and thus, frequency-dependent circuit parameters can be computed in the whole frequency band to provide an accurate description of the real structure. Finally, providing closed-form formulas is simple for lossy TLs. Without loss of generality, consider Figure 2 as the desired circuit model. The impedance matrices of sub-cells are:

$$\mathbf{Z}^{(k)} = \begin{bmatrix} Z_s^{(k)} + 1/Y_p^{(k)} & 1/Y_p^{(k)} \\ 1/Y_p^{(k)} & Z_s^{(k)} + 1/Y_p^{(k)} \end{bmatrix},$$

$$k = 1, 2, \tag{26}$$

which can be obtained from full-wave simulation. Following the parameter extraction strategy proposed in [2], it can be concluded that:

$$R^{(1)} = \mathrm{Re}\left\{ Z_s^{(1)} \right\}, \tag{27a}$$

$$L_s^{(1)} = \frac{1}{j2\omega}\left(j \cdot \mathrm{Im}\left\{ Z_s^{(1)} \right\} + \omega \frac{\partial Z_s^{(1)}}{\partial \omega} \right), \tag{27b}$$

$$C_s^{(1)} = \frac{j\omega}{2}\left(j \cdot \mathrm{Im}\left\{ Z_s^{(1)} \right\} - \omega \frac{\partial Z_s^{(1)}}{\partial \omega} \right)^{-1}, \tag{27c}$$

$$G^{(1)} = \mathrm{Re}\left\{ Y_p^{(1)} \right\}, \tag{27d}$$

$$C_p^{(1)} = \frac{1}{\omega}\mathrm{Im}\left\{ Y_p^{(1)} \right\}, \tag{27e}$$

and:

$$R^{(2)} = \mathrm{Re}\left\{ Z_s^{(2)} \right\}, \tag{28a}$$

$$L_s^{(2)} = \frac{1}{\omega}\mathrm{Im}\left\{ Z_s^{(2)} \right\}, \tag{28b}$$

$$G^{(2)} = \mathrm{Re}\left\{ Y_p^{(2)} \right\}, \tag{28c}$$

$$C_p^{(2)} = \frac{1}{j2\omega}\left(j \cdot \mathrm{Im}\left\{ Y_p^{(2)} \right\} + \omega \frac{\partial Y_p^{(2)}}{\partial \omega} \right), \tag{28d}$$

$$L_p^{(2)} = \frac{j\omega}{2}\left(j \cdot \mathrm{Im}\left\{ Y_p^{(2)} \right\} - \omega \frac{\partial Y_p^{(2)}}{\partial \omega} \right)^{-1}. \tag{28e}$$

Other variants of the circuit model can be used in which a Π-network is replaced for each sub-cell. In this study, 9-cell CRLH TL, which is similar to the one presented in [2,3], was analyzed using different methods to validate the claims made in this section. The corresponding unit-cell in microstrip implementation is depicted in Figure 3. The used substrate in this research is Rogers RT/duroid 5880 with the dielectric constant of $\varepsilon_r = 2.2$, thickness of $h = 62$ mil, and loss-tangent of $tg\delta = 0.0009$. The first and second
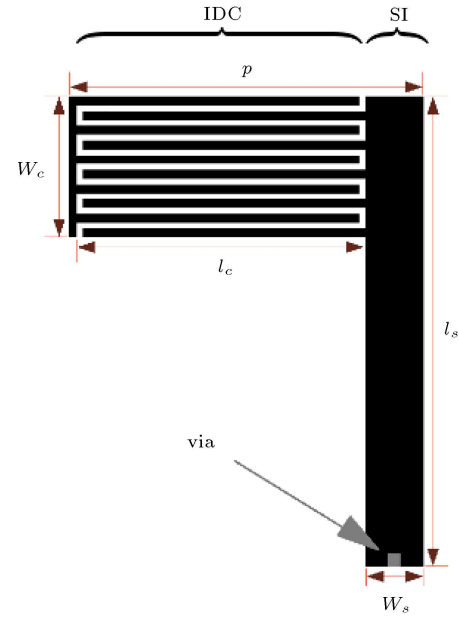

Figure 3. Unit cell of the microstrip CRLH TL: $p = 6.05$ mm, $l_c = 4.8$ mm, $w_c = 2.4$ mm, $l_s = 8.0$ mm, $w_s = 1.0$ mm, width of digits 0.15 mm, and all spacings 0.1 mm.

sub-cells correspond to IDC and SI, respectively. The approximate circuit simulations are based on the parameter values reported in [2] including $L_R = 2.45$ nH, $C_R = 0.50$ pF, $L_L = 3.38$ nH, and $C_L = 0.68$ pF at $f_0 = 3.9$ GHz. The accurate circuit simulations are based on Eqs. (27) and (28) with the extracted parameters reported in Figure 4. As expected from the small value of the substrate loss-tangent, the extracted loss parameters are too small. Note that in the proposed approach, parameters L_R, C_R, L_L, and C_L cannot be defined in a strict sense. However, in case we assume the T-network in the circuit model of IDC and SI, we can obtain their approximate values as:

$$L_R \cong 2\left(L_s^{(1)} + L_s^{(2)} \right), \tag{29a}$$

$$C_R \cong C_p^{(1)} + C_p^{(2)}, \tag{29b}$$

$$L_L \cong L_p^{(2)}, \tag{29c}$$

$$C_L \cong \frac{1}{2}C_s^{(1)}. \tag{29d}$$

In the case of the problem under study, we have $L_R = 2.23$ nH, $C_R = 0.49$ pF, $L_L = 3.36$ nH, and $C_L = 0.70$ pF at $f_0 = 3.9$ GHz. The corresponding relative errors with respect to the previously reported values are 9%, 2%, 0.6%, and 2.9%, respectively.

The attenuation constant and transmission characteristic are reported in Figures 5 and 6, respectively, which clearly show the superiority of the accurate model to its conventional counterpart that approximately fits the real structure. In these figures, "App"
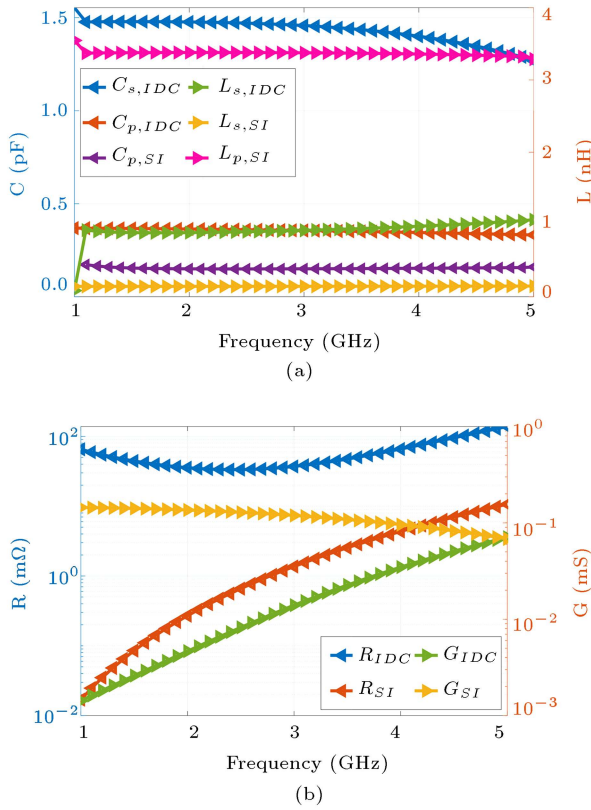
Figure 4. Extracted parameters of the CRLH unit-cell using the proposed method: (a) reactive elements and (b) lossy elements.
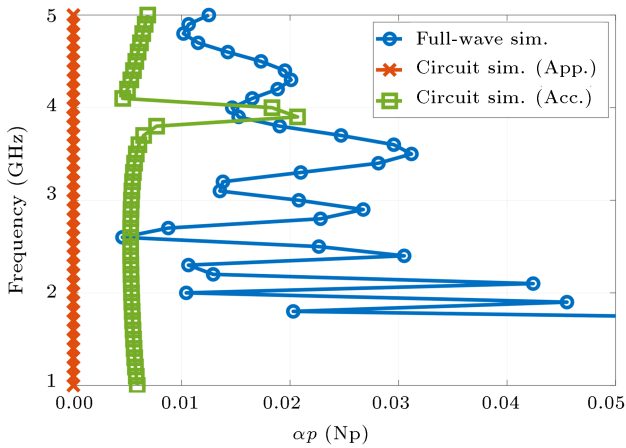

Figure 5. Attenuation constant of a 9-cell CRLH TL.

and "Acc" stand for "Approximate" and "Accurate", respectively. The difference in the computed attenuation constant based on different methods results from its negligible value and common round-off error in full-wave simulation. Perfect match between the full-wave and circuit simulations is quite impossible since mutual coupling between sub-cells of each unit cell and different unit cells are not included in the circuit model. Note that parameter extraction for each sub-cell must be carried out separately. All attempts
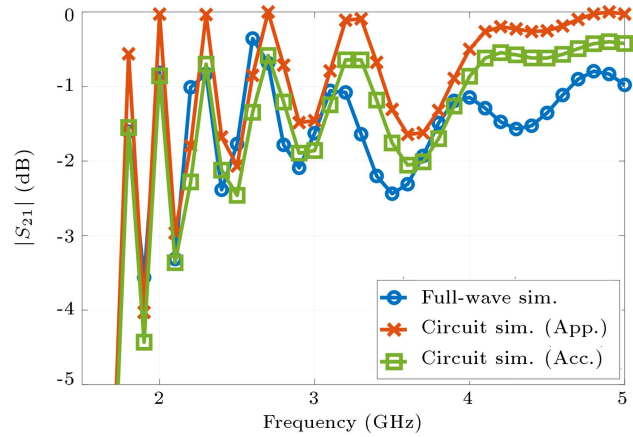

Figure 6. Transmission characteristics of a 9-cell CRLH TL.

made in this study to extract the circuit parameters from the combined unit cell failed probably due to the resonance nature of the whole unit cell. Instead, it is suitable to modify all of the matrices describing the unit cell so as to satisfy both symmetry and reciprocity criteria. Although the real structure is both symmetric and reciprocal, the obtained network representation from the full-wave simulation may not exactly satisfy these properties due to the numerical error. It can be beneficial to use averaging, whenever possible. In other words, replace z_{11} and z_{22} with $(z_{11} + z_{22})/2$ and similarly, z_{12} and z_{21} with $(z_{12} + z_{21})/2$.

5. Revisiting parameter extraction of CRLH symmetric couplers

In [3], the CRLH TLs theory was extended to a symmetric edge coupler. A complete analysis was reported which was validated by both full-wave simulation and measurement. All of the simplifying assumptions pointed out in the previous section were used for developing the circuit model. However, all the parameter extraction details were not included in this study. The coupling parameters were extracted through curve-fitting. It is worth mentioning that switching to curve-fitting violates the purpose of the circuit model for two main reasons. First, it is generally time-consuming and second, it may degrade the phase response. Note that the value of the circuit model for a coupler is considerably larger than that of an isolated TL since the full-wave analysis of the former is significantly more time-consuming than that of the latter. As a result, an easily accessible and accurate circuit model can speed up the designing and optimization of the CRLH couplers.

In the present section, the aforementioned deficiencies are eliminated. Figure 7 demonstrates the circuit model of the unit cell for the symmetric coupler, in which the first and second sub-cells include IDCs and SIs of parallel branches of the coupler unit-cell.
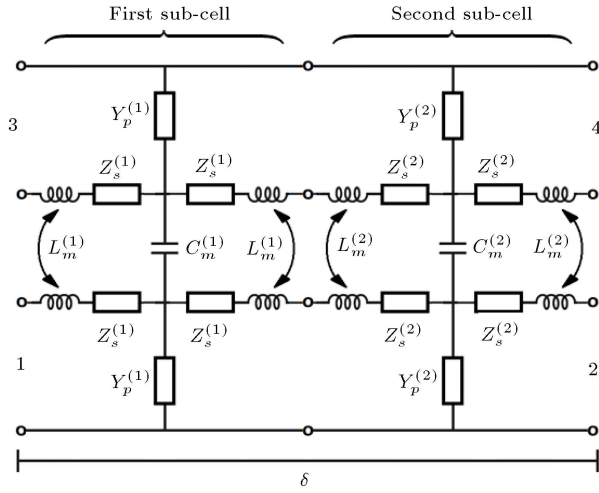
Figure 7. Circuit model of the unit cell for the symmetric edge coupler.

Here, $C_m^{(k)}$ and $L_m^{(k)}$ provide the electric and magnetic coupling, respectively. Obviously, the systematic method for analysis of this structure is even-odd mode decomposition [16], which makes it possible to use the analysis formulas of an isolated CRLH TL by properly modifying the unit cell immittances [3]. The circuit model of the TL corresponding to the even mode is the same as the one depicted in Figure 2, where $L_s^{(k)}$ is replaced by $L_s^{(k)} + L_m^{(k)}$ for $k = 1, 2$. Similarly, the circuit model of the odd mode is the same as the one depicted in Figure 2, where $C_p^{(k)}$ is replaced by $C_p^{(k)} + C_m^{(k)}$ for $k = 1, 2$. Note that compared to an isolated TL, one new parameter is added to each of the mentioned even and odd TL circuit models, i.e., coupling inductors and coupling capacitors. Likewise, the addition of the corresponding unknowns was the main reason behind using carve fitting methods for parameter extraction in [3]. If we assume that the common parameters in both even and odd modes have equal values, it is still possible to extract all the circuit parameters analytically. For instance, since the total series inductance of the first sub-cell in even and odd TLs is $L_s^{(1)} + 2L_m^{(1)}$ and $L_s^{(1)}$, respectively, computation of $L_m^{(1)}$ is trivial, assuming that $L_s^{(1)}$ in the even mode equals $L_s^{(1)}$ in the odd mode. The physical explanation of the aforementioned assumption for inductances is based on the fact that establishment of even and odd modes results from reversing the direction of the current flow. Note that the value of the self-inductance depends on the magnitude of the magnetic field encircling the line, which is independent of the current direction. Therefore, it can be concluded that both series and parallel inductances have the same values in both even and odd modes. A similar explanation can be devised for capacitances. To validate our claim, the extracted parameters of the sub-cells of the coupler with the unit cell proposed in [3] are reported
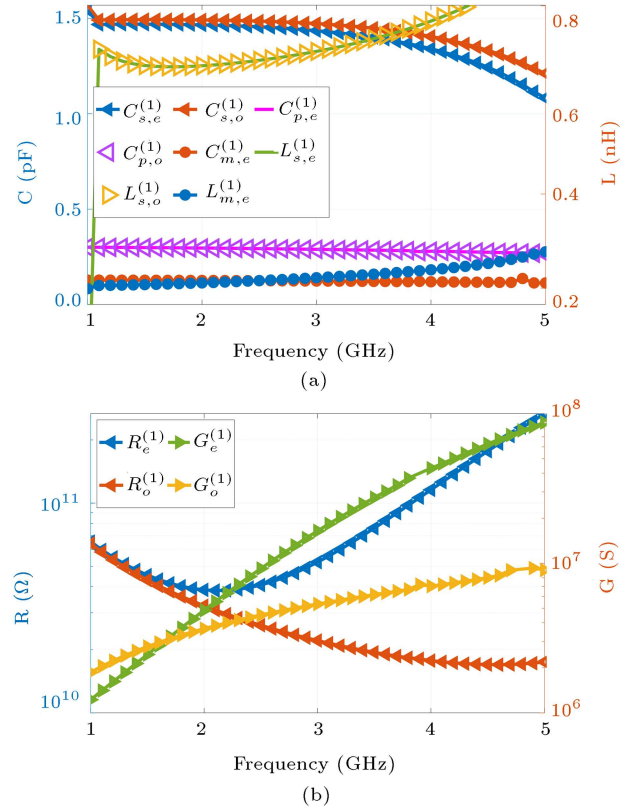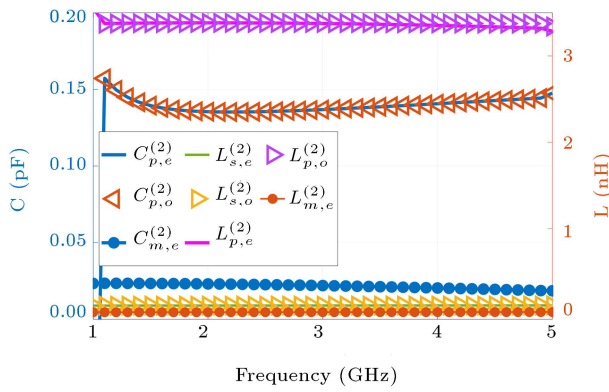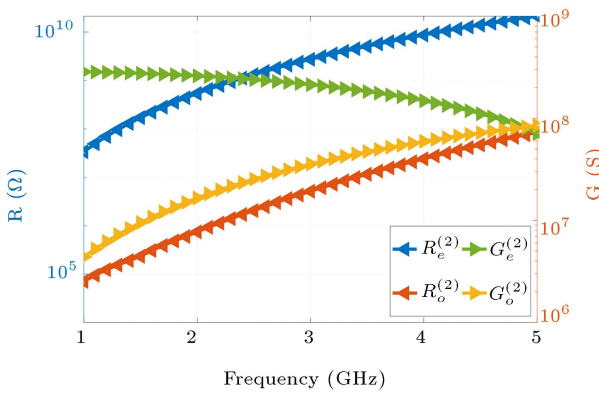

Figure 8. Extracted parameters of the first sub-cell for even and mode TLs: (a) reactive elements and (b) lossy elements.

in Figures 8 and 9, in which the subscripts "e" and "o" stand for "even" and "odd", respectively. The physical model of the complete 9-cell CRLH coupler is depicted in Figure 10 where the IDCs and SIs are all the same as those depicted in Figure 3 with the same microstrip substrate. Of note, the spacing between the parallel branches is 0.3 mm. As observed, the values of the reactive parameters are essentially the same in both even and odd modes. However, loss parameters differ significantly in different modes. Despite using a low loss substrate for microstrip realization of the coupler, loss parameters take huge values mainly due to even-odd mode decomposition. Similar to the case of an isolated TL, the parameters of each sub-cell were separately extracted. In addition, both symmetry and reciprocity conditions together with averaging are imposed on simulation results.

Figure 11 lists the S-parameters computed through full-wave and circuit simulations, which are in good agreement. However, the results of the circuit simulations reported in [3] are not included, given the author's failure to regenerate them based on the reported model parameters (some typos can be likely detected in [3].). Note that expecting "excellent agreement" is not realistic due to various couplings among the components of the unit cell, which are not included in the circuit model, i.e., coupling between

Figure 9. Extracted parameters of the second sub-cell for even and odd modes: (a) reactive elements and (b) lossy elements.
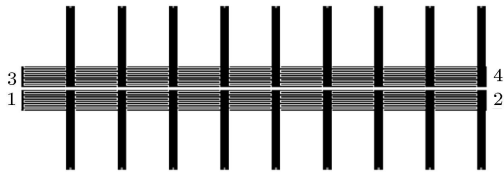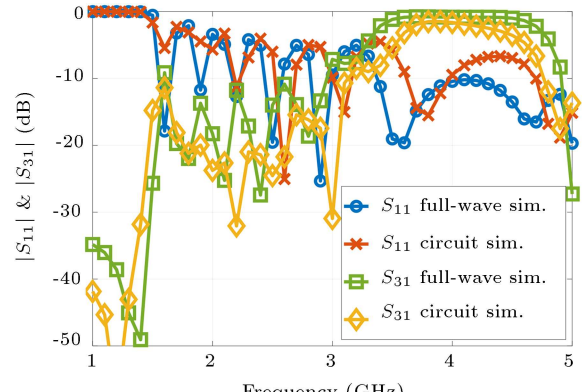

Figure 10. Physical model of the 9-cell microstrip CRLH edge coupler.

Figure 11. S-parameters of the CRLH coupler: (a) $|S_{11}|$ & $|S_{31}|$ and (b) $|S_{21}|$ & $|S_{41}|$.

fitting methods and instead, using analytic expressions solely.
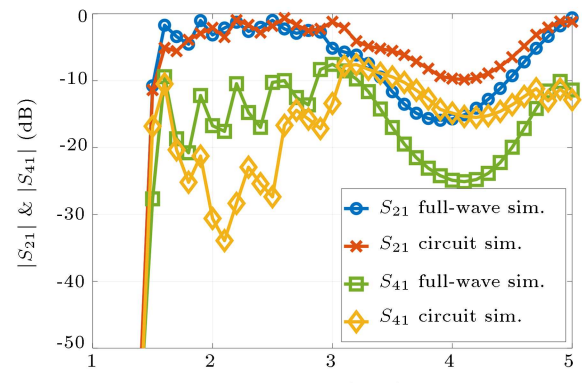
the sub-cells of each branch of the coupler and cross-couplings between sub-cells of different branches. It should be noted that the circuit parameters obtained in [3] were not in good agreement. While the two sets of S-parameters ($|S_{21}|$ and $|S_{31}|$) are in very good agreement, the two other sets ($|S_{11}|$ and $|S_{41}|$) are far apart.

6. Conclusion

Complete and unambiguous presentation of Composite Right-/Left-Handed (CRLH) Transmission Lines (TLs) is possible only when loss parameters are taken into account. Lossless CRLH TLs can be well described as the limiting case of lossy TLs. Development of an accurate circuit model for both CRLH TLs and couplers was made possible without exploiting curve

References

1. Caloz, C. and Itoh, T. "Novel microwave devices and structures based on the transmission line approach of meta-materials", *IEEE MTT-S Int. Symp.*, Philadelphia, USA, pp. 195–198 (2003).

2. Caloz, C. and Itoh, T., *Electromagnetic Metamaterials*, Wiley-IEEE Press (2006).

3. Caloz, C., Sanada, A., and Itoh, T. "A novel composite right-/left-handed coupled-line directional coupler with arbitrary coupling level and broad bandwidth", *IEEE Trans. Microw. Theory Tech.*, **52**(3), pp. 980–992 (2004).

4. Casares-Miranda, F.P., Camacho-Penalosa, C., and Caloz C. "High-gain active composite right/left-handed leaky-wave antenna", *IEEE Trans. Antennas Propag.*, **54**(8), pp. 2292–2300 (2006).

5. Mao, S. and Wu, M. "A novel 3-dB directional coupler with broad bandwidth and compact size using composite right/left-handed coplanar waveguides", *IEEE Microw. Wirel. Compon. Lett.*, **17**(5), pp. 331–333 (2007).

6. Selvanayagam, M. and Eleftheriades, G.V. "Negative-

refractive-index transmission lines with expanded unit cells", *IEEE Trans. Antennas Propag.*, **56**(11), pp. 3592–3596 (2008).

7. Lai, C., Chiu, S., Li, H., et al. "Zeroth-order resonator antennas using inductor-loaded and capacitor-loaded CPWs", *IEEE Trans. Antennas Propag.*, **59**(9), pp. 3448–3453 (2011).

8. Kim, D. and Lee, J. "Beam scanning leaky-wave slot antenna using balanced CRLH waveguide operating above the cutoff frequency", *IEEE Trans. Antennas Propag.*, **61**(5), pp. 2432–2440 (2013).

9. Chi, P. and Liu, C. "Novel dual-band quasi-0-dB coupled-line coupler using the composite right/left-handed transmission lines", *IEEE Trans Compon Packaging Manuf Technol*, **4**(2), pp. 259–267 (2014).

10. Ma, Z.L., Jiang, L.J., Gupta, S., et al. "Dispersion characteristics analysis of one dimensional multiple periodic structures and their applications to antennas", *IEEE Trans. Antennas Propag.*, **63**(1), pp. 113–121 (2015).

11. Qamar, Z., Zheng, S.Y., Chan, W.S., et al. "An equal-length multiway differential metamaterial phase shifter", *IEEE Trans. Microw. Theory Tech.*, **65**(1), pp. 136–146 (2017).

12. Bemani, M., Nikmehr, S., and Fozi, M. "A dual-band feed network for series-fed antenna arrays using extended composite right/left-handed transmission lines", *IEEE Trans. Antennas Propag.*, **65**(1), pp. 178–189 (2017).

13. Che, B.J., Jin, T., Erni, D., et al. "Electrically controllable composite right/left-handed leaky-wave antenna using liquid crystals in PCB technology", *IEEE Trans. Compon. Packaging Manuf. Technol.*, **7**(8), pp. 1331–1342 (2017).

14. Ren, D., Choi, J.H., and Itoh, T. "Series feed networks for dual-polarized frequency scanning phased array antenna based on composite right/left-handed transmission line", *IEEE Trans. Microw. Theory Tech*, **65**(12), pp. 5133–5143 (2017).

15. Yan, S. and Vandenbosch, G.A.E. "Low-profile dual-band pattern diversity patch antenna based on composite right/left-handed transmission line", *IEEE Trans. Antennas Propag.*, **65**(6), pp. 2808–2815 (2017).

16. Shen, G., Che, W., Xue, Q., et al. "Characteristics of dual composite right/left-handed unit cell and its applications to bandpass filter design", *IEEE Trans. Circuits Syst. II Express Briefs*, **65**(6), pp. 719–723 (2018).

17. Liu, F.X., Wang, Y., Zhang, S.P., et al. "Design of compact tri-band gysel power divider with zero-degree composite right-/left-hand transmission lines", *IEEE Access*, **7**, pp. 34964–34972 (2019).

18. Yang, X., Xiao, J., Wang, J., et al. "Compact frequency reconfigurable antennas based on composite right/left-handed transmission line", *IEEE Access*, **7**, pp. 131663–131671 (2019).

19. Ueda, T., Kubo, Y., Kaneda, T., et al. "Dispersion-free and tunable nonreciprocities in composite right-/left-handed metamaterials and their applications to beam squint reduction in leaky-wave antennas", *IEEE Trans. Microw. Theory Tech.*, **67**(6), pp. 2227–2237 (2019).

20. Chen, S.L., Karmokar, D.K., Li, Z., et al. "Continuous beam scanning at a fixed frequency with a composite right-/left-handed leaky-wave antenna operating over a wide frequency band", *IEEE Trans. Antennas Propag.*, **67**(12), pp. 7272–7284 (2019).

21. Szymanski, L. and Grbic, A. "2-D circuit-based bianisotropic omega media", *IEEE Trans. Antennas Propag.*, **68**(11), pp. 7395–7405 (2020).

22. Debabrata, K.K., Guo, Y.J., Chen, S.L., et al. "Composite right/left-handed leaky-wave antennas for wide-angle beam scanning with flexibly chosen frequency Range", *IEEE Trans. Antennas Propag.*, **68**(1), pp. 100–110 (2020).

23. Caloz, C. and Itoh, T. "Lossy transmission line metamaterials", *Microw. Opt. Technol. Lett.*, **43**(2), pp. 112–114 (2004).

24. Harrington, R.F., *Time-Harmonic Electromagnetic Fields*, Wiley-IEEE Press (2001).

25. Pozar, D.M., *Microwave Engineering*, John Wiley & Sons, Inc. (2012).

Biography

Babak Honarbakhsh was born in Tehran, Iran in 1981. He received his BSc, MSc, and PhD degrees in Electrical Engineering from Amirkabir University of Technology (Tehran Polytechnic) in 2004, 2007, and 2012, respectively. He is currently an Assistant Professor at the Department of Electrical Engineering at Shahid Beheshti University. His research interest is numerical electromagnetics.